

Less is More: Learning from Synthetic Data with Fine-grained Attributes for Person Re-Identification

Suncheng Xiang^{1*}, Guanjie You², Mengyuan Guan¹, Hao Chen¹,
Feng Wang¹, Ting Liu¹, Yuzhuo Fu¹

¹School of Electronic Information and Electrical Engineering, Shanghai Jiao Tong University, China

²College of Intelligence Science and Technology, National University of Defense Technology, China

{xiangsuncheng17, gemini.my, 958577057, shuipinglantian, louisa.liu, yzfu}@sjtu.edu.cn, ygjssxz@163.com

Abstract

Person re-identification (re-ID) plays an important role in applications such as public security and video surveillance. Recently, learning from synthetic data, which benefits from the popularity of synthetic data engine, has attracted attention from both academia and the public eye. However, existing synthetic datasets are limited in quantity, diversity and realism, and cannot be efficiently used for generalizable re-ID problem. To address this challenge, we construct and label a large-scale synthetic person dataset named *FineGPR* with fine-grained attribute distribution. Moreover, aiming to fully exploit the potential of *FineGPR* and promote the efficient training from millions of synthetic data, we propose an attribute analysis pipeline AOST to learn attribute distribution in target domain, then apply style transfer network to eliminate the gap between synthetic and real-world data and thus is freely deployed to new scenarios. Experiments conducted on benchmarks demonstrate that *FineGPR* with AOST outperforms (or is on par with) existing real and synthetic datasets, which suggests its feasibility for re-ID and proves the proverbial *less-is-more* principle. We hope this fine-grained dataset could advance research towards re-ID in real scenarios. Our codes and dataset will be made publicly available at <https://github.com/JeremyXSC/FineGPR>.

Introduction

Given a query image, person re-identification aims to match images of the same person across non-overlapping camera views, which has attracted lots of interests and attention in both academia and industry. Encouraged by the remarkable success of deep learning networks (He et al. 2016; Pan et al. 2018) and the availability of re-ID datasets (Ristani et al. 2016; Zheng et al. 2015), performance of person re-ID has been significantly boosted and made great progress. However, in practice, manually labelling a large diversity of training data is time-consuming and labor-intensive when directly deploying re-ID system to new scenarios. During intensive annotation, one needs to associate a pedestrian across different cameras, which is a difficult and laborious process as people might exhibit very different appearances in different cameras. In addition, there also has been an increasing concern over privacy and data security, which

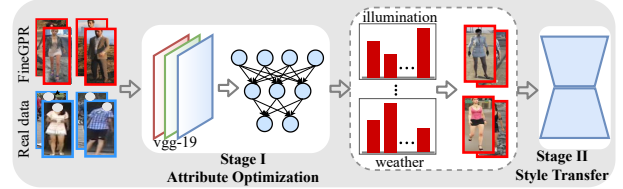


Figure 1: System workflow of the AOST method, which is based on the dataset with fine-grained attribute annotations.

makes collection of large real datasets difficult. Currently the largest real re-ID dataset, Person30K (Bai et al. 2021), which is collected with enormous labor but still lack of multiple attribute annotations. To this end, it remains challenging to find a real-world dataset that is diverse in various aspects.

To address this challenge, several works (Bak, Carr, and Lalonde 2018; Barbosa et al. 2018; Sun and Zheng 2019; Wang, Liao, and Shao 2020) have proposed to employ off-the-shelf game engines to generate synthetic person images. For example, Barbosa et al. (Barbosa et al. 2018) construct a SOMAset which contains 50 3D human models. SyRI (Bak, Carr, and Lalonde 2018) provides 100 virtual humans rendered with 140 HDR environment maps. Wang et al. (Wang, Liao, and Shao 2020) collect a RandPerson dataset with 1,801,816 synthesized person images. Although these datasets provide considerable benefits of the data scale and enable some preliminary research in person re-ID, they are quite limited in both the attribute distribution and collected environment, *e.g.*, SyRI does not have concept of cameras, and SOMAset is uniformly distributed along an environment with clothing variations. In essence, these synthetic datasets either focus on independent attribute, or require annotators to carefully simulate specific scenes in detail, few datasets consider fine-grained attribute annotations or image resolution, which limits their scalability and diversity in terms of synthesized person. Importantly, previous methods mainly focus on achieving competitive performance with large-scale data at the sacrifice of expensive time costs and intensive human labors, while neglect to perform efficient training from millions of synthetic data. Another challenge we can observe is that, existing real-world datasets can be very different in terms of content and style, *e.g.*, Market (Zheng et al. 2015) consists mostly of summer scenes

*This research was supported by the National Natural Science Foundation of China under Project (Grant No. 61977045).

Dataset		#Ids (ID-Attributes?)	#Bboxes	#Cameras	#Wea.	#Illum.	#Scenes	#Resolution
Real	Market-1501 (Zheng et al. 2015)	1,501 (✓)	32,668	6	✗	✗	✗	low
	CUHK03 (Li et al. 2014)	1,467 (✗)	14,096	2	✗	✗	✗	low
	DukeMTMC-reID (Ristani et al. 2016)	1,404 (✓)	36,411	8	✗	✗	✗	low
	MSMT17 (Wei et al. 2018)	4,101 (✗)	126,441	15	✗	✗	✗	vary
Synthetic	SOMASet (Barbosa et al. 2018)	50 (✗)	100,000	250	✗	✗	✗	–
	SyRI (Bak, Carr, and Lalonde 2018)	100 (✗)	1,680,000	280	✗	140	✗	–
	PersonX (Sun and Zheng 2019)	1,266 (✗)	273,456	6	✗	✗	1	vary
	Unreal (Zhang et al. 2021)	3,000 (✗)	120,000	34	✗	✗	1	low
	RandPerson (Wang, Liao, and Shao 2020)	8,000 (✗)	1,801,816	19	✗	✗	4	low
	<i>FineGPR (Ours)</i>	1,150 (✓)	2,028,600	36	7	7	9	high

Table 1: Comparison of some real-world and synthetic person re-ID datasets. In particular, “#Wea.”, “#Illum.” and “#Scenes” indicate whether dataset has human-annotated labels in terms of weather, illumination and background attributes, respectively.

captured in campus, while weather in the Duke (Ristani et al. 2016; Zheng, Zheng, and Yang 2017) covers a wide range of winter scenes, directly using whole *FineGPR* for training will undoubtedly produce negative effects for domain adaptation, which makes it infeasible in practical scenarios.

In order to alleviate the problems identified above and facilitate the study of re-ID community, we start from two perspectives, namely data and methodology. From the aspect of the data, we propose to collect data from synthetic world on the basis of GTA5 game engine, and manually construct a large-scale synthetic person re-ID dataset called *FineGPR*, which provides fine-grained and accurately configurable annotations, *e.g.*, viewpoint, weather, diverse and informative illumination and background, as well as the various pedestrian attribute annotations at the identity level. Compared to existing person re-ID datasets, *FineGPR* is explicitly distinguished in richness, quality and diversity. It is worth noting that our data synthesis engine is still extendable to generate more data, which can be edited/extended not only for this study, but also for future research in re-ID community.

From the aspect of methodology, we introduce a novel Attribute Optimization and Style Transfer pipeline AOST to select an upgraded version of *FineGPR* which approximates the attribute distribution in a specific real-world domain. The framework of our method can be illustrated in Fig. 1. Specifically, the proposed AOST framework contains Stage-I (*Attribute Optimization*) and Stage-II (*Style Transfer*). Firstly, attribute optimization is adopted to mine the attribute distribution of real domain, following by the style transfer network to reduce the intrinsic gap between synthetic and real domain. Finally, the transferred data are adopted for performing training on downstream vision task. This is the first time as far as we know, to greatly promote efficient training from millions of synthetic data on re-ID.

Our contribution can be summarized into three aspects:

- We construct the largest synthetic person dataset with fine-grained attributes and annotations manually for the first time in re-ID without privacy concerns.
- A two-stage pipeline AOST is proposed to learn attribute distribution which approximates the data in real domain, then eliminates style differences between synthetic and real photos.
- Extensive experiments conducted on benchmarks show

that our *FineGPR* is promising and can achieve competitive performance with AOST in re-ID task.

Related Works

Person re-ID Methods

In the field of person re-ID, early works (Zhao, Ouyang, and Wang 2014; Liao et al. 2015) either concentrate on hand-crafted feature or low-level semantic feature. Unfortunately, these methods always fail to produce competitive results because of their limited discriminative learning ability. Recently, benefited from the advances of deep neural networks, person re-ID performance in supervised learning has been significantly boosted to a new level (Wang et al. 2016; Chen et al. 2017; Li, Zhu, and Gong 2018), which learned robust feature extraction and reliable metric learning in an end-to-end manner. Typically, person re-ID model can be trained with the identification loss (Xiao et al. 2017), contrastive loss (Varior, Haloi, and Wang 2016; Varior et al. 2016) and triplet loss (Hermans, Beyer, and Leibe 2017). Recently, a strong baseline (Luo et al. 2019) for re-ID is employed to extract the discriminative feature, which proved to be having great potential to learn a robust and discriminative model in person re-ID models. Besides, several literatures (Deng et al. 2018; Xiang et al. 2020) focus on the image-level to allow different domains to have similar feature distributions, or adopt an adversarial domain adaptation approach to mitigate the distribution shift (Ganin and Lempitsky 2015; Torralba and Efros 2011), which have attracted increasing attention.

Person re-ID Datasets

Being the foundation of more sophisticated re-ID techniques, the pursuit of better datasets never stops in the area of person re-ID. Early attempts could be traced back to VIPeR (Gray, Brennan, and Tao 2007), ETHZ (Schwartz and Davis 2009) and RAiD (Das, Chakraborty, and Roy-Chowdhury 2014). More challenging datasets are proposed subsequently, including Market-1501 (Zheng et al. 2015), DukeMTMC-reID (Ristani et al. 2016; Zheng, Zheng, and Yang 2017), MSMT17 (Wei et al. 2018), *etc.* However, labelling such a large-scale real-world dataset is labor-intensive and time-consuming, sometimes there even exists security and privacy problems. Besides, all of these datasets



Figure 2: The proposed *FineGPR* dataset. **TOP**: With the same characters in different scenes, in each scene, a person can face toward a manually denoted direction. **BOTTOM**: Different characters in the same scene (*i.e.* **Scene #6**).

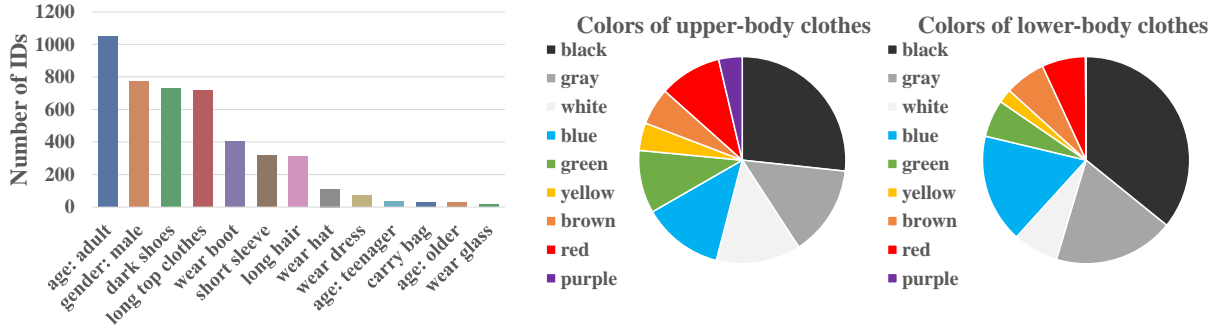


Figure 3: The distributions of attributes at the identity level on *FineGPR*. The left figure shows the numbers of IDs for each attribute. The middle and right pies illustrate the distribution of the colors of upper-body and low-body clothes respectively.

only have limited attribute distribution and are lack of diversity. As the performance gain is gradually saturated on the above datasets, newly large-scale datasets are needed urgently to further boost re-ID performance. Recently, leveraging synthetic data is an effective idea to alleviate the reliance on large-scale real-world datasets. This strategy has been applied in various computer vision tasks, *e.g.*, object detection (Pepik et al. 2012), crowd counting (Wang et al. 2019) and semantic segmentation (Chen et al. 2019). In the person re-ID community, many re-ID methods (Barbosa et al. 2018; Bak, Carr, and Lalonde 2018; Sun and Zheng 2019; Wang, Liao, and Shao 2020) have proposed to take advantage of game engine to construct large-scale synthetic re-ID datasets, which can be used to pre-train or fine-tune CNN network. For example, Barbosa et al. (Barbosa et al. 2018) propose a synthetic dataset SOMAset created by photo-realistic human body generation software to enrich the diversity. Recently, Wang et al. (Wang, Liao, and Shao 2020) collect a virtual dataset RandPerson with 3D characters containing 1,801,816 synthetic images of 8,000 identities. However, all these datasets are in a small scale, and provide limited attribute distribution, which cannot satisfy the need for generalizable person re-ID.

Approaches

Dataset Collection

In this part, we introduce a large-scale synthetic dataset named *FineGPR* with fine-grained annotations, which is col-

lected from a popular game engine called the Grand Theft Auto V (GTA5). Practically, we create a synthetic controllable world containing 2,028,600 synthesized person images of 1,150 identities. Images in this dataset generally contain different attributes in a large scope, *e.g.*, *Viewpoint*, *Weather*, *Illumination*, *Background* and ID-level annotations, also including some person images with occlusion. It is worth mentioning that all images are simultaneously captured by 36 non-overlapping cameras with a high resolution and image quality. In the process of image generation, each person walks along a schedule route, and cameras are set up and fixed at the chosen locations. As a controllable system, it can satisfy various data requirements in a fine-grained fashion.

Properties of *FineGPR* dataset

Identities. As shown by the comparison in Table 1, *FineGPR* contains 1,150 hand-crafted identities including females and males, with resolution of 200×480 . To ensure diversity, we cropped human region with different angles. As shown in Fig. 2 (Bottom), different person has different body shape, clothing, hairstyle, and the motion can be randomly set as walking, running, standing and so on. Particularly, the clothes of these characters include jeans, pants, shorts, skirts, T-shirts, dress shirts, *etc.*, and some of these identities have a backpack, shoulder bag, and wear glasses or hat. In total, we manually annotate the *FineGPR* with 13 different pedestrian attributes at the identity level (*e.g.*, wearing dress or not), the distribution diagram is demonstrated in

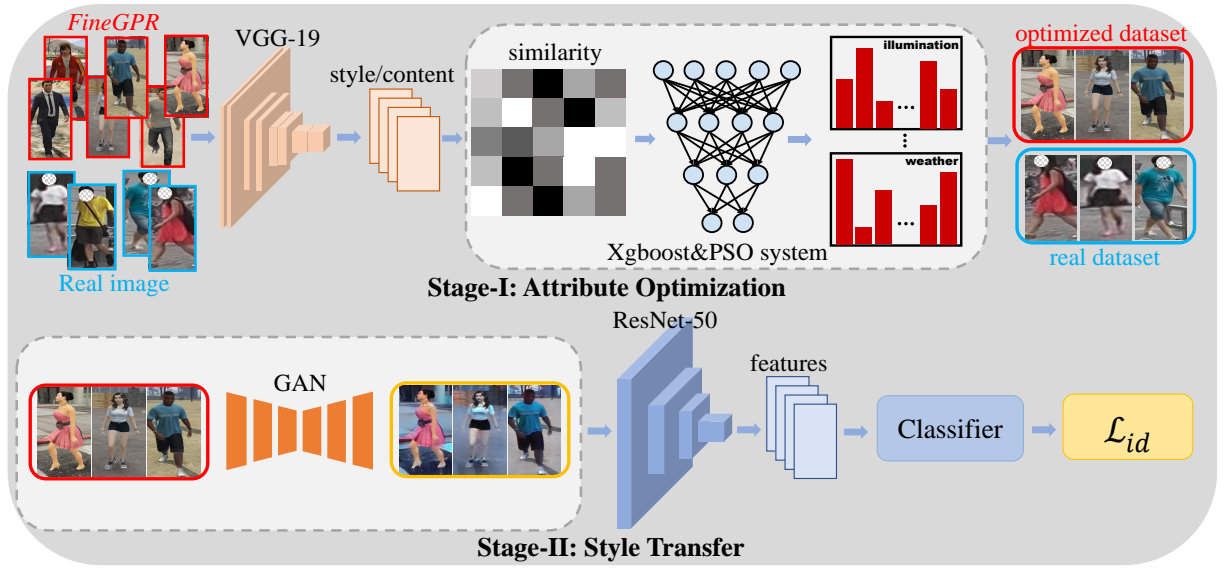


Figure 4: The two-stage pipeline **AOST** to learn attribute distribution of target domain. Firstly, we learn attribute distribution of real domain on the basis of XGBoost & PSO learning system. Secondly, we perform style transfer to enhance the reality of optimal dataset. Finally, the transferred data are adopted for downstream re-ID task.

Fig. 3.

Viewpoint. We construct the image exemplars under specified viewpoints. Those images are randomly sampled during normal walking, running, *etc.* Formally, a person image is sampled every 10° from 0° to 350° . (36 different types of viewpoints in total). There are 49 images for each viewpoint of an identity in the entire *FineGPR*, so each person has 1,764 (49×36) images in total.

Weather. Currently, the proposed *FineGPR* has 7 different weather conditions, including Sunny, Clouds, Overcast, Foggy, Neutral, Blizzard and Snowlight. It is worth mentioning that the number of instances in each weather condition is the same, but not a natural heavy-tail distribution, which makes it adaptable to various real-world scenarios.

Illumination. Illumination is another critical factor that contributes to the success of generalizable re-ID, which consists of 7 different types of illumination, *e.g.* midnight (time period during 23:00–4:00 in 24 hours a day.), dawn (4:00–6:00), forenoon (6:00–11:00), noon (11:00–13:00), afternoon (13:00–18:00), dusk (18:00–20:00) and night (20:00–23:00). Parameters like time setting can be modified manually for each illumination type. By editing the values of these terms, various kinds of illumination environments can be created.

Background. GTA5 has a very large environment map, including thousands of realistic urban areas and wild scenes. From now, 9 different scenes are selected to represent real-world scenarios with annotations, *e.g.* street, mall, school, park and mountain, *etc.*, which are distributed evenly across all identities. The different scenes are shown in Fig. 2 (Top).

The goal of our *FineGPR* dataset is to introduce a new challenging benchmark with high-quality annotations and multiple attribute distribution to re-ID community. To the best of our knowledge, this is the first synthetic person re-ID

dataset with over 4 environment-level attributes and 13 ID-level attribute annotations. More additional details related to our *FineGPR* can be found in the **Supplementary Material**.

Methodology of Proposed AOST

In this section, we design an effective training strategy AOST to directly select samples on the basis of synthetic *FineGPR* for initializing the re-ID backbone. And the overall framework is illustrated in Fig. 4, which includes two stages: Attribute Optimization and Style Transfer.

Attribute Optimization Intuitively, since *FineGPR* is a large-attribute-range dataset, using entire *FineGPR* for training is time-consuming and low-efficient. To further exploit the potential of *FineGPR* and promote the training efficiency, we introduce a novel strategy to learn some representative attributes with prior target knowledge. Following the procedure in (Gatys, Ecker, and Bethge 2016), we adopt a widely used backbone VGG-19 (Simonyan and Zisserman 2014) pre-trained on ImageNet (Deng et al. 2009) to obtain the style distance $\mathcal{D}_{\text{style}}$ and content distance $\mathcal{D}_{\text{content}}$ respectively, which are formulated as:

$$\mathcal{D}_{\text{content}} = \frac{1}{2} \sum_{i,j} (F_{ij}^l - P_{ij}^l)^2 \quad (1)$$

$$\mathcal{D}_{\text{style}} = \sum_{l=0}^L w_l \frac{1}{4N_l^2 M_l^2} \sum_{i,j} (G_{ij}^l - A_{ij}^l)^2 \quad (2)$$

where F_{ij}^l and P_{ij}^l denote representations extracted by VGG-19. w_l is a hyper-parameter that controls the importance of each layer to the style. N_l represents the number of filters and M_l is size of the feature map. G_{ij} and A_{ij} denote the Gram Matrix of real and synthetic images in layer

Algorithm 1: The Proposed AOST Method

Input: Labeled synthetic data L ; Unlabeled real target data U ;
Initialized VGG model ϕ ; Xgboost model θ_0 ;
Two hyper-parameters α and β ; Iteration rounds n ;
Output: Best re-ID model $f(w, x_i)$

- 1: Initialize: $m = 1, iter = 1$;
- 2: \triangleright *Attribute Optimization* ***
- 3: Extract \mathcal{D}_{style} & $\mathcal{D}_{content}$ between L and U with model ϕ ;
- 4: $\mathcal{D}_{total} \leftarrow \alpha * \mathcal{D}_{style} + \beta * \mathcal{D}_{content}$;
- 5: **while** $m \leq \|U\|$ **do**
- 6: Optimized model $\theta^* \leftarrow$ train θ_0 with L and \mathcal{D}_{total} ;
- 7: Optimized attributes $\mathcal{V}^* \leftarrow$ update θ^* with PSO;
- 8: Update the sample size: $m \leftarrow m + 1$;
- 9: **end while**
- 10: Generate a new dataset L^* according to \mathcal{V}^* ;
- 11: \triangleright *Style Transfer* ***
- 12: Performing style transfer with GAN on L^* ;
- 13: **if** $iter \leq n$ **then**
- 14: Initializing re-ID model with L^* by softmax loss ;
- 15: $iter \leftarrow iter + 1$;
- 16: **end if**

l . Then total distance for attribute metric is represented as

$$\mathcal{D}_{total} = \alpha * \mathcal{D}_{style} + \beta * \mathcal{D}_{content} \quad (3)$$

where α and β are two hyper-parameters which control the relative importance of style and content distance respectively. As depicted in Alg. 1, a tree boosting system named XGBoost (Chen and Guestrin 2016) model θ_0 is trained with *FineGPR* and \mathcal{D}_{total} . Based on the upgraded Xgboost model θ^* , we continuously adopt a widely used Particle Swarm Optimization (PSO) (Kennedy and Eberhart 1995) method to search some optimized attributes. Typically, it selects a similar style or content distribution with respect to a real target dataset. The optimization framework can be shown in Fig. 4 (Stage I). To our knowledge this is the first demonstration to perform attribute optimization with large-scale synthetic dataset on person re-ID task. In essence, compared with existing methods for attribute optimization, such as reinforcement learning (Ruiz, Schultze, and Chandraker 2018) and attribute descent (Yao et al. 2020), our method investigates and learns these attribute distributions only with few parameters to optimize, which makes it more flexible and adaptable.

Style Transfer In the above attribute optimization stage, there exists serious domain gap or distribution shift between synthetic and real-world scenario. Generative Adversarial Networks (GAN) (Goodfellow et al. 2014) which have demonstrated impressive results on image-to-image translation seem to be a natural solution to this problem. However, existing methods are both inefficient and ineffective in practical application. Their inefficiency results from the fact that a new generator needs to be retrained when given a new real-world scenario. Meanwhile, these methods mainly employ low-resolution images to train a generator, and they are incapable of fully exploiting the potential of GAN, which is likely to limit the quality of generated images. To provide a remedy to this dilemma, we build a high-resolution dataset MSCO and crawled over 20K images with a size of nearly 200×480 from MSMT17 (Wei et al. 2018) and COCO (Lin



Figure 5: Some visual examples of our MSCO dataset.

et al. 2014). Different locations are also considered to cover a large diversity. We believe that a unified dataset with high-resolution can provide more useful information during translation. Some visual examples of collected MSCO dataset are illustrated in Fig 5. By doing so, we only need to train one generator and translate the synthetic images into photo-realistic style at testing phase. The details can be seen in Fig. 4 (Stage II). To verify the priority of MSCO, we adopt several state-of-the-art methods for style-level domain adaptation, e.g., CycleGAN (Zhu et al. 2017), PTGAN (Wei et al. 2018) and SPGAN (Deng et al. 2018).

Experiments

Datasets and Evaluation

Market-1501 (Zheng et al. 2015) contains 32,668 labeled images of 1,501 identities captured from campus in Tsinghua University. Each identity is captured by at most 6 cameras. It is divided into training set and test set. The training set contains 12,936 images from 751 identities and the test set contains 19,732 images from 750 identities.

DukeMTMC-reID (Ristani et al. 2016; Zheng, Zheng, and Yang 2017) is collected from Duke University with 8 cameras, it has 36,411 labeled images belonging to 1,404 identities and contains 16,522 training images from 702 identities, 2,228 query images from another 702 identities and 17,661 gallery images.

CUHK03 (Li et al. 2014) contains 14,097 images of 1,467 identities. Following the CUHK03-NP protocol (Zhong et al. 2017), it is divided into 7,365 images of 767 identities as the training set, and the remaining 6,732 images of 700 identities as the testing set. We adopt mean Average Precision (mAP) and Cumulative Matching Characteristics (CMC) at rank-1 and rank-5 for evaluation on re-ID task.

Experiment Settings

We mainly use the newly-built *FineGPR* to conduct the experiments. For attribute optimization, we empirically set $w_l = 0.2$ in Eq. 2, and $\alpha = 0.9, \beta = 1$ in Eq. 3. It is worth mentioning that our re-ID baseline system is built only with commonly used softmax cross-entropy loss (Zhang and Sabuncu 2018) on vanilla ResNet-50 (He et al. 2016) with no bells and whistles. Following the practice in (Luo et al. 2019), person images are resized to 256×128 , then a random horizontal flipping with 0.5 probability is used for data augmentation. The batch size of training samples is set as 128. Adam method (Kingma and Ba 2014) is adopted for optimization. The initial learning rate is set to 3.5×10^{-4} for the backbone network. Then, these learning rates are decayed to 3.5×10^{-5} and 3.5×10^{-6} at 40th epoch and 70th epoch respectively, and the training stops after 120 epochs.

Testing set →		Market-1501			DukeMTMC-reID			CUHK03		
Training set ↓	Synthetic data	Rank-1	Rank-5	mAP	Rank-1	Rank-5	mAP	Rank-1	Rank-5	mAP
Market-1501 (Zheng et al. 2015)	×	<u>92.7</u>	<u>97.9</u>	<u>81.4</u>	19.3	32.0	10.0	5.3	12.4	6.2
DukeMTMC-reID (Ristani et al. 2016)	×	40.4	57.8	17.4	<u>84.9</u>	<u>92.9</u>	<u>72.5</u>	4.8	11.5	5.4
CUHK03 (Li et al. 2014)	×	36.6	53.9	16.6	14.2	25.8	6.9	<u>43.6</u>	<u>62.9</u>	<u>41.5</u>
SOMAs [*] (Barbosa et al. 2018)	✓	4.5	—	1.3	4.0	—	1.0	0.4	—	0.4
SyRI [*] (Bak, Carr, and Lalonde 2018)	✓	29.0	—	10.8	23.7	—	9.0	4.1	—	3.5
Unreal [‡] (Zhang et al. 2021)	✓	37.4	55.2	15.9	22.9	37.3	12.2	4.3	10.0	4.7
PersonX [*] (Sun and Zheng 2019)	✓	44.0	—	20.4	35.4	—	18.1	7.4	—	6.2
RandPerson [*] (Wang, Liao, and Shao 2020)	✓	55.6	—	28.8	47.6	—	27.1	13.4	—	10.8
<i>FineGPR</i> (Ours)	✓	50.5	67.7	24.6	35.5	50.3	18.1	8.7	18.2	8.4
<i>FineGPR</i> +AOST (Ours)	✓	56.3	70.4	29.2	47.5	54.8	27.0	14.2	20.6	11.2

Table 2: Performance comparison with existing Real and Synthetic datasets on Market-1501, DukeMTMC-reID and CUHK03, respectively. **Red** indicates the best and **Blue** the second best. * means results are reported by RandPerson (Wang, Liao, and Shao 2020). [‡] represents results reproduced with Unreal_v2.1 on our baseline. Underline denotes supervised learning.



Figure 6: Some visual examples selected by the attribute optimization on different datasets. Each group surrounded by the red box is the similar pair mined by our model.

Comparison with the State-of-the-arts

To evaluate the superiority of our synthetic dataset, we perform training on *FineGPR* and testing on each individual real dataset. The evaluation results are reported in Table 2. Interestingly, when initializing with whole *FineGPR* dataset, we can achieve a rank-1 accuracy of **50.5%**, **35.5%** and **8.7%** when tested on Market-1501, DukeMTMC-reID and CUHK03 respectively. When compared with RandPerson (Wang, Liao, and Shao 2020), our *FineGPR*+AOST can lead a significant improvement by **+0.7%** and **+0.8%** in rank-1 accuracy on Market-1501 and CUHK03 dataset respectively. When compared with real-world datasets, *FineGPR* also outperforms these benchmarks by an impressively large margin in terms of rank-1 accuracy, leading **+10.1%** and **+13.9%** improvement on Market-1501 compared with DukeMTMC-reID and CUHK03 separately. However, initializing with whole *FineGPR* dataset is time-consuming and low-efficient, this motivates the investigation of data filter techniques that can potentially address this problem.

Ablation Study

In order to prove the effectiveness of individual technical contributions, we perform the following ablation study.

Effectiveness of attribute optimization We proceed study on dependency by testing whether the Attribute Optimization (AO) matters. According to Table 3, our at-

tribute optimization strategy (*FineGPR*+ AO (w/o transfer)) can lead a significant improvement in rank-1 of **+5.6%**, **+5.2%** and **+2.6%** on Market-1501, DukeMTMC-reID and CUHK03 respectively when compared with random sampling (*FineGPR*+Random). We suspect this is due to samples selected by attribute optimization strategy are much closer to real target domain, and the learned attribute distribution has a higher quality, which have a direct impact on downstream re-ID task. Meanwhile, fast training is our second main advantage since the scale of training set can be largely decreased by attribute optimization. *e.g.*, it costs nearly 20 GPU-days¹ when pre-training on entire *FineGPR* with 2,028,600 images. However, training time will be considerably reduced by **15×** (20 vs. 1.3 GPU-days) by our proposed AOST without performance degradation, which leads a more efficient deployment to real-world scenarios. Surprisingly, Even with fewer samples for training, our approach still yields its competitiveness when compared with existing methods, *e.g.* 56.3% vs. 55.6% in rank-1 on Market, proving the proverbial *less-is-more* principle.

Effectiveness of style transfer Though our synthetic *FineGPR* can achieve a satisfactory performance in most cases for generalizable re-ID task, it is still not as good as RandPerson (Wang, Liao, and Shao 2020) where 132,145 person images of 8,000 identities are adopted for training. We suspect that the success of RandPerson can be largely attributed to the huge number of identities, which can greatly enhance the discrimination capability of backbone network. Note that for fairness, we instead consider an easier but practical strategy, that is, employing off-the-shelf style transfer model to generate photo-realistic images for further effective training. As shown in Table 3, *w/o* style transfer by AOST, the rank-1 accuracy drops sharply from 56.3% to 45.5% and the mAP drops from 29.2% to 23.8%. The final performances show that mitigating domain gap between synthetic and real dataset is crucial to make the performance to an excellent level. For simplicity, the SPGAN is used as the style transfer model in the following experiments.

¹All timings use one Nvidia Tesla P100 GPU on a server equipped with a Intel Xeon E5-2690 V4 CPU.

Testing set →			Market-1501			DukeMTMC-reID			CUHK03		
Training set ↓	Bboxes	Time (days) ↓	Rank-1	Rank-5	mAP	Rank-1	Rank-5	mAP	Rank-1	Rank-5	mAP
<i>FineGPR</i>	2,028,600	20	50.5	67.7	24.6	35.5	50.3	18.1	8.7	18.2	8.4
<i>FineGPR</i> +Random	124,200	1.3	39.9	57.1	18.3	20.9	35.2	10.4	5.9	15.4	5.4
<i>FineGPR</i> +AO (w/o transfer)	124,200	1.3	45.5	63.2	23.8	26.1	42.2	17.3	8.5	16.9	8.3
<i>FineGPR</i> +AOST (Ours)	124,200	1.3	56.3	70.4	29.2	47.5	54.8	27.0	14.2	20.6	11.2

Table 3: Controlled experiments by different regulations of our proposed AOST method on Market-1501, DukeMTMC-reID and CUHK03, respectively. “Random” indicates random sampling, “AO” means Attribute Optimization.



Figure 7: Qualitative comparisons of different GAN methods when trained on Market and our MSCO, respectively.

Qualitative and Quantitative Results

Qualitative evaluations To further validate the effectiveness of our attribute optimization method, we present some visual exemplars qualitatively *w.r.t* different real target datasets. As shown in Fig. 6, it can be obviously observed that the selected samples from *FineGPR* are more similar to the real target samples in terms of style and content representation. In addition, Fig. 7 presents a visual comparison of different transfer methods on original low-resolution dataset Market and high-resolution dataset MSCO respectively. It can be easily noticed that GANs create artifacts and coarse results (indicated by **yellow box**) when trained on low-resolution images, which still remains problematic. In comparison, our method with MSCO can successfully address the artifacts and produce most visually pleasant results (indicated by **red box**) in an even better fashion, which is implicitly beneficial to the downstream re-ID mission.

Quantitative evaluations Our qualitative observations above are confirmed by the quantitative evaluations. To be more specific, we adopt Fréchet Inception Distance (FID) (Heusel et al. 2017) to measure the distribution difference between synthetic and real photos. Generally, FID measures how close the distribution of generated images is to the real. As shown in Fig. 8, by adding new regulation terms, *e.g.* attribute optimization or style transfer, the FID score gradually decreases no matter which dataset is employed for evaluation, suggesting the learned attribute distributions are more and more similar to the real images. Even prior to this point, according to Fig. 9, training a generator with low-resolution images always produce low-quality images

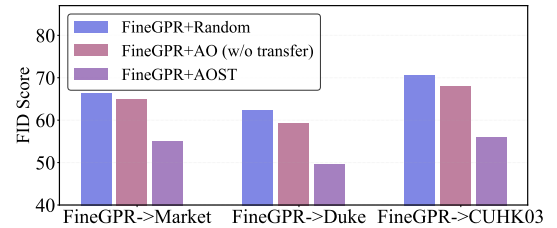


Figure 8: Comparison of FID (lower is better) to evaluate the effectiveness of different regulation terms of AOST.

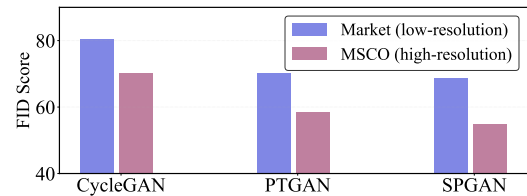


Figure 9: Comparison of FID (lower is better) to evaluate the realism of generated images by CycleGAN, PTGAN and SPGAN when trained on samples with different resolution.

(indicated by higher FID score) no matter which style transfer model is employed. Still, SPGAN and PTGAN rank the best, while SPGAN shows a slight quantitative advantage. In all, the introduction of high-resolution MSCO dataset can always improve the adaptability to style changes and mitigate previously mentioned domain gap effectively, even in much more complex scenarios.

Conclusion & Future Work

In this work, we construct a large-scale person dataset *FineGPR* with fine-grained attribute labels, which differs from existing synthetic datasets in multiple aspects, *e.g.* various attribute distributions and high-quality annotations. On top of *FineGPR*, we introduce an attribute analysis methodology called AOST to learn important attribute distribution, which enjoys the benefits of small-scale dataset for more efficient training, continuously, style transfer is adopted to further mitigate domain gap between synthetic and real photos. With this, we proved, for the first time, that a model trained on limited synthetic data can yield a competitive performance in generalizable re-ID task. Extensive experiments

also demonstrate the superiority of *FineGPR* and effectiveness of AOST. In the future, we will continue to enrich our dataset and hope its role will shed light into potential tasks for the community to move forward.

Broader Impacts and Ethical Considerations

Our dataset and method can help to advance the research of person re-ID, thus promoting the development of smart city and security systems in the future metropolises. However, when applying re-ID technology to identify pedestrians in surveillance systems, it may lead to leakage of person's privacy or personal information since re-ID systems often rely on large scale pedestrian datasets for training. Some security companies may also use this technology to track pedestrians through cameras without their consent, so governments and officials need to carefully establish strict regulations and laws to control the usage of re-ID technologies.

As for ethical considerations, for example, people-centric datasets pose some challenges of intersectional accuracy disparities (Buolamwini and Gebru 2018). In view of this, our task and dataset were created with careful attention to ethical questions, which we encountered throughout our work. Access to our dataset will be provided for research purposes only and with restrictions on redistribution. Additionally, as we filtered out the sensitive attribute name in our fine-grained attribute annotation, our dataset cannot be easily repurposed for unintended tasks. Importantly, we are very cautious of human-annotation procedure of large scale datasets towards the social and ethical implications. Furthermore, we do not consider the datasets for developing non-research systems without further processing or augmentation. We hope this fine-grained dataset will shed light into potential tasks for the research community to move forward.

References

- Bai, Y.; Jiao, J.; Ce, W.; Liu, J.; Lou, Y.; Feng, X.; and Duan, L.-Y. 2021. Person30K: A Dual-Meta Generalization Network for Person Re-Identification. In *Proceedings of the IEEE/CVF Conference on Computer Vision and Pattern Recognition*, 2123–2132.
- Bak, S.; Carr, P.; and Lalonde, J.-F. 2018. Domain adaptation through synthesis for unsupervised person re-identification. In *Proceedings of the European Conference on Computer Vision (ECCV)*, 189–205.
- Barbosa, I. B.; Cristani, M.; Caputo, B.; Rognhaugen, A.; and Theoharis, T. 2018. Looking beyond appearances: Synthetic training data for deep cnns in re-identification. *Computer Vision and Image Understanding*, 167: 50–62.
- Buolamwini, J.; and Gebru, T. 2018. Gender shades: Intersectional accuracy disparities in commercial gender classification. In *Conference on fairness, accountability and transparency*, 77–91. PMLR.
- Chen, T.; and Guestrin, C. 2016. Xgboost: A scalable tree boosting system. In *Proceedings of the 22nd acm sigkdd international conference on knowledge discovery and data mining*, 785–794.
- Chen, W.; Chen, X.; Zhang, J.; and Huang, K. 2017. Beyond triplet loss: a deep quadruplet network for person re-identification. In *Proceedings of the IEEE conference on computer vision and pattern recognition*, 403–412.
- Chen, Y.; Li, W.; Chen, X.; and Gool, L. V. 2019. Learning semantic segmentation from synthetic data: A geometrically guided input-output adaptation approach. In *Proceedings of the IEEE/CVF Conference on Computer Vision and Pattern Recognition*, 1841–1850.
- Das, A.; Chakraborty, A.; and Roy-Chowdhury, A. K. 2014. Consistent re-identification in a camera network. In *European conference on computer vision*, 330–345. Springer.
- Deng, J.; Dong, W.; Socher, R.; Li, L.-J.; Li, K.; and Fei-Fei, L. 2009. Imagenet: A large-scale hierarchical image database. In *2009 IEEE conference on computer vision and pattern recognition*, 248–255. Ieee.
- Deng, W.; Zheng, L.; Ye, Q.; Kang, G.; Yang, Y.; and Jiao, J. 2018. Image-image domain adaptation with preserved self-similarity and domain-dissimilarity for person re-identification. In *Proceedings of the IEEE conference on computer vision and pattern recognition*, 994–1003.
- Ganin, Y.; and Lempitsky, V. 2015. Unsupervised domain adaptation by backpropagation. In *International conference on machine learning*, 1180–1189. PMLR.
- Gatys, L. A.; Ecker, A. S.; and Bethge, M. 2016. Image style transfer using convolutional neural networks. In *Proceedings of the IEEE conference on computer vision and pattern recognition*, 2414–2423.
- Goodfellow, I.; Pouget-Abadie, J.; Mirza, M.; Xu, B.; Warde-Farley, D.; Ozair, S.; Courville, A.; and Bengio, Y. 2014. Generative adversarial nets. *Advances in neural information processing systems*, 27.
- Gray, D.; Brennan, S.; and Tao, H. 2007. Evaluating appearance models for recognition, reacquisition, and tracking. In *Proc. IEEE international workshop on performance evaluation for tracking and surveillance (PETS)*, volume 3, 1–7. Citeseer.
- He, K.; Zhang, X.; Ren, S.; and Sun, J. 2016. Deep residual learning for image recognition. In *Proceedings of the IEEE conference on computer vision and pattern recognition*, 770–778.
- Hermans, A.; Beyer, L.; and Leibe, B. 2017. In defense of the triplet loss for person re-identification. *arXiv preprint arXiv:1703.07737*.
- Heusel, M.; Ramsauer, H.; Unterthiner, T.; Nessler, B.; and Hochreiter, S. 2017. Gans trained by a two time-scale update rule converge to a local nash equilibrium. *Advances in neural information processing systems*, 30.
- Kennedy, J.; and Eberhart, R. 1995. Particle swarm optimization. In *Proceedings of ICNN'95-international conference on neural networks*, volume 4, 1942–1948. IEEE.
- Kingma, D. P.; and Ba, J. 2014. Adam: A method for stochastic optimization. *arXiv preprint arXiv:1412.6980*.
- Li, W.; Zhao, R.; Xiao, T.; and Wang, X. 2014. Deepreid: Deep filter pairing neural network for person re-identification. In *Proceedings of the IEEE conference on computer vision and pattern recognition*, 152–159.

- Li, W.; Zhu, X.; and Gong, S. 2018. Harmonious attention network for person re-identification. In *Proceedings of the IEEE conference on computer vision and pattern recognition*, 2285–2294.
- Liao, S.; Hu, Y.; Zhu, X.; and Li, S. Z. 2015. Person re-identification by local maximal occurrence representation and metric learning. In *Proceedings of the IEEE conference on computer vision and pattern recognition*, 2197–2206.
- Lin, T.-Y.; Maire, M.; Belongie, S.; Hays, J.; Perona, P.; Ramanan, D.; Dollár, P.; and Zitnick, C. L. 2014. Microsoft coco: Common objects in context. In *European conference on computer vision*, 740–755. Springer.
- Luo, H.; Gu, Y.; Liao, X.; Lai, S.; and Jiang, W. 2019. Bag of tricks and a strong baseline for deep person re-identification. In *Proceedings of the IEEE/CVF Conference on Computer Vision and Pattern Recognition Workshops*, 0–0.
- Pan, X.; Luo, P.; Shi, J.; and Tang, X. 2018. Two at once: Enhancing learning and generalization capacities via ibn-net. In *Proceedings of the European Conference on Computer Vision (ECCV)*, 464–479.
- Pepik, B.; Stark, M.; Gehler, P.; and Schiele, B. 2012. Teaching 3d geometry to deformable part models. In *2012 IEEE conference on computer vision and pattern recognition*, 3362–3369. IEEE.
- Ristani, E.; Solera, F.; Zou, R.; Cucchiara, R.; and Tomasi, C. 2016. Performance measures and a data set for multi-target, multi-camera tracking. In *European conference on computer vision*, 17–35. Springer.
- Ruiz, N.; Schuster, S.; and Chandraker, M. 2018. Learning to simulate. *arXiv preprint arXiv:1810.02513*.
- Schwartz, W. R.; and Davis, L. S. 2009. Learning discriminative appearance-based models using partial least squares. In *2009 XXII Brazilian symposium on computer graphics and image processing*, 322–329. IEEE.
- Simonyan, K.; and Zisserman, A. 2014. Very deep convolutional networks for large-scale image recognition. *arXiv preprint arXiv:1409.1556*.
- Sun, X.; and Zheng, L. 2019. Dissecting person re-identification from the viewpoint of viewpoint. In *Proceedings of the IEEE/CVF Conference on Computer Vision and Pattern Recognition*, 608–617.
- Torralba, A.; and Efros, A. A. 2011. Unbiased look at dataset bias. In *CVPR 2011*, 1521–1528. IEEE.
- Varior, R. R.; Haloi, M.; and Wang, G. 2016. Gated siamese convolutional neural network architecture for human re-identification. In *European conference on computer vision*, 791–808. Springer.
- Varior, R. R.; Shuai, B.; Lu, J.; Xu, D.; and Wang, G. 2016. A siamese long short-term memory architecture for human re-identification. In *European conference on computer vision*, 135–153. Springer.
- Wang, F.; Zuo, W.; Lin, L.; Zhang, D.; and Zhang, L. 2016. Joint learning of single-image and cross-image representations for person re-identification. In *Proceedings of the IEEE Conference on Computer Vision and Pattern Recognition*, 1288–1296.
- Wang, Q.; Gao, J.; Lin, W.; and Yuan, Y. 2019. Learning from synthetic data for crowd counting in the wild. In *Proceedings of the IEEE/CVF Conference on Computer Vision and Pattern Recognition*, 8198–8207.
- Wang, Y.; Liao, S.; and Shao, L. 2020. Surpassing real-world source training data: Random 3d characters for generalizable person re-identification. In *Proceedings of the 28th ACM International Conference on Multimedia*, 3422–3430.
- Wei, L.; Zhang, S.; Gao, W.; and Tian, Q. 2018. Person transfer gan to bridge domain gap for person re-identification. In *Proceedings of the IEEE conference on computer vision and pattern recognition*, 79–88.
- Xiang, S.; Fu, Y.; You, G.; and Liu, T. 2020. Unsupervised domain adaptation through synthesis for person re-identification. In *2020 IEEE International Conference on Multimedia and Expo (ICME)*, 1–6. IEEE.
- Xiao, T.; Li, S.; Wang, B.; Lin, L.; and Wang, X. 2017. Joint detection and identification feature learning for person search. In *Proceedings of the IEEE Conference on Computer Vision and Pattern Recognition*, 3415–3424.
- Yao, Y.; Zheng, L.; Yang, X.; Naphade, M.; and Gedeon, T. 2020. Simulating content consistent vehicle datasets with attribute descent. In *Computer Vision—ECCV 2020: 16th European Conference, Glasgow, UK, August 23–28, 2020, Proceedings, Part VI 16*, 775–791. Springer.
- Zhang, T.; Xie, L.; Wei, L.; Zhuang, Z.; Zhang, Y.; Li, B.; and Tian, Q. 2021. UnrealPerson: An Adaptive Pipeline towards Costless Person Re-identification. In *Proceedings of the IEEE/CVF Conference on Computer Vision and Pattern Recognition*, 11506–11515.
- Zhang, Z.; and Sabuncu, M. R. 2018. Generalized cross entropy loss for training deep neural networks with noisy labels. In *32nd Conference on Neural Information Processing Systems (NeurIPS)*.
- Zhao, R.; Ouyang, W.; and Wang, X. 2014. Learning mid-level filters for person re-identification. In *Proceedings of the IEEE conference on computer vision and pattern recognition*, 144–151.
- Zheng, L.; Shen, L.; Tian, L.; Wang, S.; Wang, J.; and Tian, Q. 2015. Scalable person re-identification: A benchmark. In *Proceedings of the IEEE international conference on computer vision*, 1116–1124.
- Zheng, Z.; Zheng, L.; and Yang, Y. 2017. Unlabeled samples generated by gan improve the person re-identification baseline in vitro. In *Proceedings of the IEEE international conference on computer vision*, 3754–3762.
- Zhong, Z.; Zheng, L.; Cao, D.; and Li, S. 2017. Re-ranking person re-identification with k-reciprocal encoding. In *Proceedings of the IEEE conference on computer vision and pattern recognition*, 1318–1327.
- Zhu, J.-Y.; Park, T.; Isola, P.; and Efros, A. A. 2017. Unpaired image-to-image translation using cycle-consistent adversarial networks. In *Proceedings of the IEEE international conference on computer vision*, 2223–2232.